# Tensile Strength Modelling of Glass Fibre-Polymer Composites in Fire

**S. Feih[1], Z. Mathys[2], A.G. Gibson[3] & A.P. Mouritz[1,*]**

*1. School of Aerospace, Mechanical & Manufacturing Engineering,*
*Royal Melbourne Institute of Technology, GPO Box 2476V, Melbourne, Victoria, 3001, Australia and*
*Cooperative Research Centre for Advanced Composite Structures Ltd (CRC-ACS),*
*506 Lorimer Street, Fishermans Bend, Victoria, 3207, Australia*

*2. Platform Sciences Laboratory, Defence Science & Technology Organisation,*
*GPO Box 4331, Melbourne, Victoria, 3001, Australia*

*3. Centre for Composite Materials Engineering, Stephenson Building,*
*University of Newcastle-upon-Tyne, United Kingdom*

[*] Corresponding author:
Tel: +61 3 9925 6269
Fax: +61 3 9925 6003
e-mail: adrian.mouritz@rmit.edu.au

**ABSTRACT**

A thermal-mechanical model is presented to calculate the tensile strength and time-to-failure of glass fibre reinforced polymer composites in fire. The model considers the main thermal processes and softening (mechanical) processes of fibreglass composites in fire that ensure an accurate calculation of tensile strength and failure time. The thermal component of the model considers the effects of heat conduction, matrix decomposition and volatile out-gassing on the temperature-time response of composites. The mechanical component of the model considers the tensile softening of the polymer matrix and glass fibres in fire, with softening of the fibres analysed as a function of temperature and heating time. The model can calculate the tensile strength of a hot, decomposing composite exposed to fire up to the onset of flaming combustion. The thermal-mechanical model is confined to hot, smouldering fibreglass composites prior to ignition. Experimental fire tests are performed on dry fibreglass fabric and fibreglass/vinyl ester composite specimens to validate the model. It is shown that the model gives an approximate estimate of the tensile strength and time-to-failure of the materials when exposed to one-sided heating at a constant heat flux. It is envisaged the model can be used to calculate the tensile softening and time-to-failure of glass-polymer composite structures exposed to fire.

**Keywords:** A. Polymer-matrix composites (PMCs), B. Thermomechanical properties. C. Modelling. Glass fibres. Fire

# 1 INTRODUCTION

The most common type of reinforcement used in polymer matrix composites is fibreglass. It is estimated that fibreglass is used in 90-95% of all composite products. Fibreglass is used in a wide range of composite products including aircraft and helicopter components, boat and ship structures, transport vehicles such as automobiles and rail carriages, electrical/electronic appliances, and many types of consumer goods. The use of fibreglass composites will grow in coming years as these materials penetrate deeper into established markets (eg. boating, transportation) and find new applications in emerging markets (eg. bridges and other civil infrastructure). However, one issue challenging the greater use of composite materials in products traditionally made using metals is their high flammability. Many composite materials, whether reinforced with glass or another fibrous material (eg. carbon), have a flammable polymer matrix that combusts at high temperature. Composites can smoulder or burn with the release of large amounts of heat, smoke and fumes that pose a serious safety hazard. Composites are also a safety risk because they can soften, buckle and collapse in a fire. This is a concern when composites are used in structural applications, such as aircraft components, ship structures and civil infrastructure such as buildings and bridges, when failure can cause injury and death.

A great deal of research has recently been published on the softening and failure of composites in fire [1-12]. Most of the research has focussed on compressive failure of fibreglass composites because of their use in structures supporting compression loads. It is well known that thermal softening, viscoelastic creep and decomposition of the polymer matrix can reduce the compressive properties of fibreglass composites in fire [6,7,11]. Two types of models are available to predict the loss in compressive strength and failure of fibreglass composites, depending on the fire temperature. The first type of model considers thermal softening and creep effects of the matrix at temperatures below the polymer decomposition temperature (which is typically between 250-400$^{o}$C) [6,5]. The other type of model considers thermal softening and decomposition (pyrolysis) of the matrix at higher temperatures [8,10-12]. Both models ignore the effect of thermal softening of the glass fibers because of the dominant influence of the polymer matrix on compressive failure.

Recent fire research by Mouritz and colleagues [10-12] has shown that tensile failure of fibreglass composites is dependent on thermal softening of both the polymer matrix and fibres. Composites retain significant tensile strength after the matrix has fully softened and decomposed because of the strength provided by the glass fibres. Failure of composites under tensile loading eventually occurs by thermal softening and rupture of the fibres. Modelling the tensile strength and failure of fibreglass composites in fire is more complicated than modelling compressive failure because softening of both the polymer matrix and fibres must be considered. Gibson et al. [10,12] and Mouritz et al [11] have proposed models to estimate the tensile failure of composites in fire, although the predictions are approximate because softening of the fibres is not adequately modelled.

This paper presents a new model for predicting the tensile strength and failure of fibreglass composites in fire. The paper is structured as follows: firstly, the thermo-mechanical model is presented in Section 2. The model considers the effect of thermal softening of the polymer matrix and glass fibres on the tensile strength in fire. Secondly, the experimental methods required to derive material values and validate the model are presented in Section 3. Tensile tests were performed on glass/vinyl ester composites subjected to one-sided heating at temperatures from ~250 to 700$^{o}$C to rigorously evaluate the model for a wide range of fire conditions. Thirdly, Section 4 presents research evaluating the accuracy of the model in predicting the tensile strength and failure of glass fibres and fibreglass composites in fire.

## 2 THERMAL-MECHANICAL MODEL

### 2.1 Background

The approach to modelling the tensile strength of fibreglass composites in fire involves thermal analysis and mechanical analysis. The thermal analysis determines the temperature profile through the composite when exposed to one-sided radiant heating. The temperature in the through-thickness direction is not uniform, but of course is highest at the heat-exposed surface and lowest at the back (unexposed) surface until thermal equilibrium is achieved. It is assumed that the tensile strength varies

in the through-thickness direction due to the temperature gradient; with the strength being lowest at the heated surface and increasing towards the back surface. By calculating the tensile strength at different locations through the composite, and then averaging these values, it is possible to determine the bulk strength. This approach makes it possible to calculate the tensile strength for any fire temperature and heating time.

The model assumes that one side of a flat composite plate is evenly heated at a constant heat flux, as shown schematically in figure 1. This simulates the radiant heating of a simple shell structure by fire. It is also assumed that a static tension stress is applied in the axial (lengthwise) direction. Using these assumptions, the composite can be modelled as a one-dimensional system where the temperature and tensile strength vary only in the through-thickness ($x$) direction. The one-dimensional nature of the model is not a drawback for most applications involving composites due to their shell-like structure. Furthermore, it is possible to expand the model to consider 2D and 3D systems, although they are not considered here. Deformation and expansion occurs in the $x$ and $y$ directions of the plate due to the one-sided heating that causes the beam to bend and elongate [8,11], however these deformations are assumed not to affect significantly the tensile properties.

### 2.2 Thermal Analysis of Composite

The model by Gibson et al. [13] is used to calculate the temperature profile through a composite plate exposed to one-sided heating. The model is based on thermal analysis of polymer composites performed earlier by Henderson et al. [14]. The model considers three important processes on the temperature of a hot decomposing composite. The first process is heat conduction from the fire/composite interface into the material, which causes the temperature to rise. The second process is heat generated or absorbed by decomposition of the polymer matrix. Polymers that decompose via exothermic reactions generate heat that causes the temperature to rise while polymers that degrade by endothermic reactions reduce the temperature. The third process is the flow of volatile gases generated by the decomposition of the polymer matrix towards the fire/composite interface. The initial temperature of the gases is lower than the temperature of the char region through which they

must flow to reach the fire/composite interface, and therefore the outflow of the volatiles has a convective cooling effect. The one-dimensional equation that considers the effect of the three processes on the temperature-time response ( $\partial T / \partial t$ ) of a composite is expressed by [13]:

$$\rho C_p \frac{\partial T}{\partial t} = \frac{\partial}{\partial x}\left( k \frac{\partial T}{\partial x} \right) - \frac{\partial M}{\partial t}\left( Q_P + h_C - h_G \right) - \dot{M}_g \frac{\partial}{\partial x} h_G \qquad (1)$$

In the equation, $T$, $t$ and $x$ are the temperature, time and through-thickness coordinates, respectively. $\rho$, $C_p$ and $k$ are the density, specific heat and thermal conductivity of the composite, and the latter two can be specified as functions of temperature. $\dot{M}_g$ is the mass flux of volatiles; $h_C$ and $h_G$ are the enthalpies of the composite and evolved gas, respectively; and $Q_p$ is the endothermic decomposition energy of the polymer matrix. The three terms on the right relate to heat conduction, resin decomposition and volatile convection, respectively. The resin decomposition term is negative when the decomposition process is endothermic and positive when exothermic. Most polymers decompose by endothermic reactions and so this term is negative in Eqn. (1). The last term is also negative because of the convective cooling effect of the volatiles.

The decomposition rate of the polymer matrix is expressed in Eqn. (1) by $\partial M / \partial t$. When the matrix decomposes by a single-stage reaction process then $\partial M / \partial t$ is calculated using the first-order Arrhenius relationship:

$$\frac{\partial M}{\partial t} = -A M_o \left( \frac{M - M_f}{M_o} \right) e^{(-E/RT)} \qquad (2)$$

where $A$ and $E$ are the rate constant and activation energy of the decomposition reaction, respectively, and these values must be measured using thermogravimetric analysis (TGA) of the polymer. $R$ is the universal gas constant. $M_o$, $M$ and $M_f$ are the original, instantaneous (at a given time) and final mass of

the polymer during the decomposition process, and these values are also determined using TGA. The model considers unit volumes, and density and mass are therefore effectively identical. The matrix density is updated through the evaluation of Eqn. (2) during the thermal analysis, and the density of the composite is calculated by rule-of-mixtures:

$$\rho_{comp} = V_f \rho_f + (1 - V_f)\rho_m \tag{3}$$

$V_f$ is the fibre volume fraction and $\rho_f$ and $\rho_m$ are the density of the fibre and matrix, respectively. The fibres are assumed to remain inert during the thermal analysis, which means that fibre mass loss is not accounted for in the model. During the calculation the values of the thermal constants of the composite and the enthalpy are continually updated to allow for the effects of resin decomposition, and the enthalpy is calculated on the basis of the instantaneous thermal constants and the temperature. $\dot{M}_g$, the mass flux of decomposition volatiles, is calculated from the change in density of the material and integrated through the thickness of the laminate to account for the build-up of these gases. The thermal model is validated against experimentally measured temperature profiles, as described in Section 4.1.

### 2.3 Tensile Strength of Polymer Matrix in Fire

Once the temperature profile has been calculated using Eqn. (1), the tensile strengths of the polymer matrix and glass fibers at different locations through the composite can be calculated from the known temperature at each location. The reduction in polymer strength with increasing temperature is outlined here. Figure 2 shows the typical relationship between the strength and temperature of a thermoset polymer. This type of relationship has been observed for many different polymer systems [10,11]. The tensile strength remains at the room temperature value, $\sigma_{m(0),}$ until it reaches a critical softening temperature ($T_{cr}$), above which the strength decreases with increasing temperature to an apparently minimum value, $\sigma_{m(R).}$ This reduction is due solely to thermal softening of the polymer as it undergoes the glassy transformation. However, the model ignores the effect of creep softening of the

matrix, which is not significant for fibreglass composites loaded in tension. The strength decreases very gradually below $\sigma_{m(R)}$ at temperatures above $T_m$ due to further visco-plastic softening and (eventually) pyrolysis of the polymer.

The curve presented in figure 2 for a typical thermoset is not perfectly symmetric around the glass transition temperature ($T_g$). In many polymer systems the strength has dropped by more than 50% before the $T_g$. However, the curve is nearly symmetric around $T_g$', the so-called mechanical glass transition temperature, defined by the temperature at which the strength has decreased by 50%. This is an important consideration in applying an analytical equation that relates matrix strength to temperature. A number of mathematical functions for analysing the symmetric behaviour around $T'_g$ were examined, and particular success was achieved with the hyperbolic *tanh* function:

$$\sigma_m(T) = \left( \frac{\sigma_{m(0)} + \sigma_{m(R)}}{2} - \frac{\sigma_{m(0)} - \sigma_{m(R)}}{2} \tanh\left(k_m\left(T - T_g^{'}\right)\right)\right) R_{rc}(T)^n \qquad (4)$$

where $T$ is the temperature calculated using Eqn. (1) and $k_m$ is an empirical constant describing the breadth of the strength-temperature curve. The modelling approach out-lined here requires *a prior* knowledge of the values of $\sigma_{m(0)}$, $\sigma_{m(R)}$, $T_g^{'}$ and $k_m$, which must be measured by experimental testing. The data are evaluated in Section 4.2.

In addition to the effect of thermal softening considered by the tanh function in Eqn. (4), it is also necessary to account for thermal decomposition of the matrix at high temperatures, a process which is assumed to further lower the resin strength. Little is currently known about the effect of pyrolysis on the mechanical properties of polymers, other than the properties are very low. Until a more appropriate relationship can be found, it is proposed that a power law factor, $R_{rc}^{\ n}$, based on the residual resin content can be used to predict the properties. $R_{rc}(T)$ is the remaining resin content during decomposition of the polymer matrix $\left(1 \geq R_{rc} \geq 0\right)$. When $R_{rc}$ equals 1, there has been no mass loss as

a result of the resin decomposition process; for $R_{rc}$ = 0 the matrix has completely volatised and there is no residual mass. Consequently, the resin strength must be zero, which is also the result of including $R_{rc}$ in Eq. (3). While Eq. (4) combines the two processes of resin softening and decomposition in one expression, both factors remain independent as their respective temperature intervals do not overlap.

The remaining mass at any temperature throughout the laminate can be calculated using Eqn. (2). The exponent $n$ is an empirical constant dependent on the relationship between mass loss and strength of the polymer matrix. When $n$ = 0 it is assumed that resin decomposition has no affect on strength, and the matrix strength equals $\sigma_{m(R)}$ for any temperature above $T_m$. When $n$ = 1 it is assumed that a linear relationship exists between mass loss and strength whereas higher values of $n$ can be used to describe non-linear relationships between mass loss and strength. Previous research by Feih et al. [15] has shown that taking $n$ = 3 gives a good estimate of compressive strength for a vinyl ester resin, and this value was used for the tensile strength analysis.

### 2.4 Tensile Strength of Glass Fibre Bundles in Fire

The tensile strength of glass fibres decreases with rising temperature and also with time at temperature. The cause of this strength reduction has been much-debated [16] and satisfactory conclusions have yet to be drawn. The available results to date, and various interpretations of them, were discussed by Gupta [16] in 1988 and there has been little new information since. The loss in strength has been attributed to various factors that may include (1) annealing of compressive residual stresses, (2) re-orientation or loss of orientation of a network structure within the glass (3) the presence of a surface layer with different properties, which may subsequently be changed and (4) development of surface flaws due to high temperature attack, probably by water. Explanation (1) has now been fairly widely discredited, but (2)-(4) are still regarded as plausible, despite little evidence of either network orientation or differences between the surface and the bulk of the material.

We do not aim to contribute here to the discussion on the mechanisms controlling fibre strength at high temperatures. No matter which mechanisms are involved, it is clear that the fracture toughness and therefore rupture strength of glass is dependent on the temperature and heating time. For this reason, the effects of both temperature and time on the tensile strength of fibre bundles are considered in the model. The typical relationship between bundle strength and temperature and time is shown in figure 3 (a). The strength decreases rapidly with increasing temperature. The strength also decreases with increasing time for a fixed elevated temperature, at least for a certain period after which the strength stabilizes at a minimum value. This behaviour occurs for any type of glass, although the amount and rate of softening is dependent on the chemical composition and residual stress state of the fibre.

There is no physically based model which can account for the reduction of glass strength at high temperatures. The complexity of the softening processes makes the development of a physically based model a challenging research problem. A phenomenological model was therefore developed based on the experimental data. The curves shown in figure 3 (a) follow a profile that can be described mathematically using a *tanh* function. In fact, several other functions can also approximate the curve profiles, however the *tanh* function is the easiest to solve. The *tanh* function that describes the relationship between fibre bundle strength $\sigma_{fb}$, temperature $T$ and heating time $t$ is:

$$\sigma_{fb}(t,T) = \sigma_{fb(0)} - \sigma_{\text{loss}}(T)\tanh\left[k_{fb}(T)t\right] \tag{5}$$

where $\sigma_{fb(0)}$ is the tensile strength at 20°C, $\sigma_{loss}(T)$ describes the strength loss, and $k_{fb}(T)$ describes the rate of strength loss as a function of temperature. $k_{fb}(T)$ is determined from a curve-fit temperature function using:

$$k_{fb}(T) = k_1 e^{k_2 T} \tag{6}$$

where $k_1$ and $k_2$ are curve-fir constants that must be determined by elevated temperature strength tests on fibres.

The strength loss function, $\sigma_{loss}(T)$, occurs in a symmetric fashion around a temperature, $T_{50\%}$. $T_{50\%}$ is the temperature at which the fibre bundle loses 50% of its tensile strength for long-term heat exposure. The strength loss is determined using:

$$\sigma_{loss}(T) = \frac{\sigma_{fb(0)}}{2} + \frac{\sigma_{fb(0)}.tanh\left[p_{fb}(T - T_{50\%})\right]}{2} \tag{7}$$

with $T_{50\%}$ and $p_{fb}$ being curve-fit constants. Knowing the dependence of fibre strength on temperature and time from experimental data, it is possible to determine values for $k_{fb}(T)$, $T_{50\%}$ and $p_{fb}$. The experimental data to derive these values for E-glass bundles is presented in Section 4.2.

### 2.5 Tensile Strength of Fibreglass Composites in Fire

The tensile strength of a fibreglass composite in fire is determined firstly by calculating the through-thickness temperature profile in time intervals. These time intervals have to be small enough to resolve the temperature profile accurately. The temperature at each location in the through-thickness direction (ie. $x_1$, $x_2$, … $x_n$ in figure 1) is determined using Eqn. (1) by averaging the temperatures at the start ($t_j$) and end ($t_j+\Delta t$) for each time interval:

$$T_{\mathrm{av,j}}(x_i) = \frac{T_{\mathrm{t_j}}(x_i) + T_{\mathrm{t_j+\Delta t}}(x_i)}{2} \tag{8}$$

$\Delta t$ is the length of the time interval. The tensile strengths of the matrix ($\sigma_m$) and fibres ($\sigma_f$) at locations $x_i$ need to be determined. The strength dependency of both matrix and fibres was established with isothermal heating conditions. The composite under fire, however, is exposed to one-sided heating that causes the temperature at any given location to increase with time until a steady-state thermal

condition is reached. The matrix strength can be calculated using Eqn. (4) as it is considered time-independent. The fibre strength degradation needs to take the increasing temperature with time into account to remain conservative, and the procedure for doing this is visualised in figure 3 (b). At room temperature, the fibre bundle strength is $\sigma_{fb(0)}$. The fibres are now exposed to an elevated temperature $T_1$ for an exposure time $t_1$. The strength $\sigma_{fb(1)}$ can be calculated for this temperature and time using Eqn. (5) (stage I). For the following time interval, the average temperature increases. For consistency during intervals, the strength at the beginning of the new time interval needs to remain the same as the strength at the end of the previous time interval ($t_{j+\Delta t}=t_{j+1}$). This can only be achieved if the exposure time $t_{j+1}$ is re-calculated to an effective exposure time, $t_{eff,j+1}$, at the start of the new interval with new temperature. The effective exposure time can be considered as the time the fibres need to be exposed to isothermal heating conditions at $T_2$ to experience the same strength degradation $\sigma_{fb(1)}$.as experienced at $T_1$. This is expressed mathematically in Eqn. (9):

$$\sigma_{fb}(t_{j+\Delta t}, T_{av(j)}) = \sigma_{fb}\left(t_{eff,j+1}, T_{av(j+1)}\right) \tag{9}$$

The calculation of $t_{eff}$ (stage II in figure 3(b)) in Eqn. (9) requires the derivation of the inverse function of Eqn. (5):

$$t_{eff,j+1}(x_i) = \frac{1}{k_f\left(T_{av(j+1)}(x_i)\right)} \operatorname{arctanh}\left[\frac{\sigma_{fb(0)} - \sigma_{fb}\left(t_{j+\Delta t}, T_{av(j)}\right)}{\sigma_{\text{loss}}\left(T_{av(j+1)}(x_i)\right)}\right] \tag{10}$$

Once $t_{eff,j+1}$ is obtained, the reduced fibre strength at each location can be calculated for the end of the time interval using the Eqn. (5) with the effective time $t_{eff}$ instead of real time $t$.

$$\sigma_{fb(j+1)}\left(T_{\text{av(j+1)}}(x_i), t_{\text{eff,j+1}}(x_i) + \Delta t\right) = \sigma_{fb(0)} - \sigma_{\text{loss}}\left(T_{\text{av(j+1)}}(x_i)\right)\tanh\left[k\left(T_{\text{av(j+1)}}(x_i)\right)\left(t_{\text{eff,j+1}}(x_i) + \Delta t\right)\right] \tag{11}$$

As the temperature increases, the effective exposure time $t_{eff}$ decreases below the real time, $t$, and becomes dependent on the location as the temperature history is different throughout the composite. It is straight-forward to calculate $t_{eff}$ with Eqn. (11) as all other variables are a function of the average interval temperature only and therefore known. The new strength value $\sigma_{fb(2)}$ calculated from Eqn. (11) is also visualised in figure 3 (b) (stage III).

The reduction to the tensile strength of the polymer matrix and glass fibres is calculated in increments of temperature and time at each location, as denoted by subscript $i$, in the through-thickness direction. From these contributions, the composite tensile strength can then be determined. The rule-of-mixtures is the most simple approach to determine the tensile strength and generally gives good estimates for unidirectional composites:

$$\sigma_{(i)}(T,t) = V_f \sigma_{fb(i)}(T,t) + (1 - V_f)\sigma_{m(i)}(T) \qquad \text{with } T < T'_g \tag{12}$$

where $V_f$ is the fibre volume fraction of the composite in load direction, $\sigma_{fb(i)}$ the fibre bundle strength and $\sigma_{m(i)}$ the matrix contribution to strength (i.e. the matrix stress at the failure strain of the fibres). In the present case, $\sigma_{m(i)}$ does not contribute much to the overall strength.

Equation (12) does not consider the load mechanics of fibrous woven composites. It is acknowledged that more advanced strength theories take fibre strength distribution, fibre waviness, progressive fibre breakage and load transfer between fibres into account to give more accurate predictions [17]; however, these models become increasingly more complex.

Elevated temperature testing shows that the composite strength reduces beyond the matrix contribution given in Eqn. (12). The 'composite effect' in which all the fibres can be considered to bear equal load is lost. When, as in woven structures, there is a possibility of 'path differences' between different

fibres this can result in uneven fibre loading, so some fibres will fail at lower composite strains than others. This effect can result, at elevated temperatures, in the actual fibre contribution to strength falling substantially below the value of the fibre term in the law-of-mixtures equation. This effect needs to be included, so we have chosen here to modify the rule-of-mixtures equation by applying an empirical 'load transfer factor', which comes into account once resin softening occurs:

$$\sigma_{(i)}(T,t) = \Phi_{LT}(T) V_f \sigma_{fb(i)}(T,t) + (1 - V_f)\sigma_{m(i)}(T) \quad with \quad \Phi_{LT}(T) \le 1, \tag{13}$$

where $\Phi_{LT}$ is the load transfer factor. The value is unity at room temperature and in that case Eqn. (13) yields the standard rule-of-mixtures (Eqn. (12)). Load transfer is reduced once the matrix starts to soften, and $\Phi_{LT}$ reduces the contribution of the glass bundle strength to the overall composite strength. The load transfer factor is assumed to reach a minimum value upon complete softening of the matrix, and its value is determined by elevated temperature testing of the composite under tensile loading. The experimental data is presented in Section 4.2.

Once the strength at various locations is known, the residual strength can be determined for each time interval by integrating through-the-thickness using Simpson integration:

$$\sigma_{\text{av}} = \frac{1}{t}\int_{-x/2}^{+x/2} \sigma\left(T_{\text{av}}(x), t_{\text{eff}}(x)\right) dx \quad \text{with} \tag{14}$$

$$\int_{-x/2}^{+x/2} \sigma\left(T(x), t_{eff}(x)\right) dx = \frac{h}{3m}\left[\sigma(T_{av}(x_0), t_{eff}(x_0)) + 4\sigma\left(T(x_1), t_{eff}(x_1)\right) + 2\sigma\left(T(x_2), t_{eff}(x_2)\right) + \ldots\right.$$

$$\left. 2\sigma\left(T(x_{k-2}), t_{\text{eff}}(x_{k-2})\right) + 4\sigma\left(T(x_{k-1}), t_{\text{eff}}(x_{k-1})\right) + \sigma\left(T(x_k), t_{\text{eff}}(x_k)\right)\right] \tag{15}$$

*m* is the number of intervals for the integration and *h* is the laminate thickness. *m* needs to be an even value for Simpson integration. This procedure for calculating the tensile strength of a fibreglass

composites exposed to one-sided heating is summarised in the flowchart in figure 4. The following sections present the experimental data to validate the proposed model.

## 3 MATERIAL & EXPERIMENTAL METHODS

### 3.1 Polymer and Dry Glass Laminates

The ability of the thermal-mechanical model to accurately determine the tensile strength of fibreglass composites in fire was evaluated using an E-glass/vinyl ester material. The composite was made using E-glass woven fabric (Owens Corning, 800 g/m$^2$) and vinyl ester resin (Derakane 411-350; Ashland Composite Polymers). The resin did not contain flame retardant fillers or additives, and had a glass transition temperature ($T_g$) of 120$^o$C. The composite was fabricated using the vacuum-bag resin infusion process, cured under ambient conditions (20ºC, 55% RH), and post-cured at 80ºC for two hours. The fibre stacking sequence of the laminate was [0/90] using 15 woven plies, and the fibre volume content was 55%.

The ability of the model to predict the tensile strength of glass fibres (in the absence of the polymer matrix) as a function of temperature and time was also evaluated. Dry glass laminates were made using the E-glass fabric (800 g/m$^2$) stacked in [0/90] pattern using 15 woven plies. The laminates contained the same type, stacking pattern and number of glass plies as the glass/vinyl ester composite.

### 3.2 High temperature Strength Testing of Fibreglass, Polymer and Composite

The tensile strength of E-glass fibre bundles was measured at different temperatures and heating times to determine the *tanh* curve fit constants of $k_{fb}(T)$ and $p_{fb}$. E-glass bundles (Owens Corning, 300 tex) were heated in a furnace at temperatures between 150ºC and 650ºC for different times up to two hours. Fibre bundles rather than single fibres were tested as the composite laminate also contains fibre bundles. No load was applied to the fibre bundles during the heat treatment to avoid creep effects. The fibre bundles were then cooled in air and tensile tested using a 10 kN Instron machine. A gauge

length of 150 mm was used for the fibre bundles. It is assumed that no strength recovery occurs when the fibres are cooled from the furnace temperature to room temperature. As found from preliminary tests, tensile tests on fibre bundles at high temperature gave similar strength values when compared to their residual strength at room temperature after exposure to the same heating conditions.

The tensile strength of the vinyl ester matrix resin was measured at temperatures up to 150ºC to determine the values for $\sigma_{m(0)}$, $\sigma_{m(R)}$, $T_g$' and $k_m$ needed to solve Eqn (4). The tests were performed according to ASTM D368-02 using rectangular polymer coupons with a gauge length of 150 mm, width of 25 mm and thickness of 4 mm.

Tensile tests were performed on the glass/vinyl ester at several temperatures between 20 and 300ºC. The tests were performed according to ASTM 3039 using coupons with a gauge length of 150 mm, width of 25 mm and thickness of 4 mm. The loss of strength up to 300ºC was attributed to loss of load transfer between fibres and used to determine $\Phi_{LT}$. Heat exposure of specimens was kept sufficiently short to minimize the loss in glass strength. All coupons were loaded in tension at a rate of 2 mm/min inside an oven (hot box) attached to a 100 kN Instron machine.

### 3.3 Fire Testing

Artificial fire tests were performed on glass/vinyl ester and glass fabric specimens to generate experimental data to validate the model. Figure 5 shows the fire-under-load test, which involves pre-loading the specimen in tension while simultaneously heating one-side using a radiant heater. A constant tensile stress between 10% and 80% of the room temperature strength was applied to the specimen using a 250 kN MTS machine. The specimen was exposed to a constant heat flux radiated from a 5000W cone-shaped heater while under the constant tensile load. (The heater is the heating device used in the cone calorimeter instrument). The specimen and heater were both in a vertical orientation and spaced 25 mm apart. The heating time taken for the specimen to fail, called the time-to-failure, was measured. Under low stress and low temperature conditions the specimen did not fail, and these tests were stopped after several hours.

The specimens were 730 mm long, 50 mm wide and 9 mm thick, although only a 100 mm long section in the centre was heated. This ensured the heat source was well away from the load cell to the MTS machine. The material outside the heated region was thermally insulated with a thermal blanket (Fiberfrax® 550K (Unifrax)). The unheated (cooler) surface of the specimen was also thermally insulated. Two specimens were tested for most heat flux/load combinations. It should be noted that the experimental restrictions required a different specimen size for the elevated temperature tests and fire-under-load tests, which leads to a size effect for the tensile strength. This is discussed in Section 4.4.

Fire-under-load tests were performed at heat fluxes of 10, 25, 50 and 75 kW/m$^2$, which generated maximum surface temperatures of about 280, 450, 600 and 800$^o$C, respectively. The tests were performed over this wide range of heat fluxes to rigorously test the model. Increasing the heat flux from 10 to 75 kW/m$^2$ caused different amounts and states of decomposition to the composite material. The lowest heat flux (10 kW/m$^2$) heated the composite to ~280$^o$C, which is well above the glass transition temperature (120$^o$C) but below the decomposition temperature (~350$^o$C) of the vinyl ester matrix. The heat flux of 25 kW/m$^2$ heated the surface to above the decomposition temperature of the matrix (450$^o$C), but due to the thermal gradient through the composite most of the underlying material did not decompose. The two highest heat fluxes caused complete decomposition of the polymer matrix, with the decomposition rate being highest at 75 kW/m$^2$.

## 4 VALIDATION OF THERMAL-MECHANICAL MODEL

### 4.1 Temperature Profiles of Composite Material

The thermal model described by Eqn. (1) is used to predict the through-thickness temperature profile for composites subjected to one-sided heating at a constant heat flux. Figure 6 shows the temperature-time curves at different locations in the glass/vinyl ester composite at heat fluxes from 10 to 75 kW/m$^2$. The thermal property data for the glass/vinyl ester given in table 1 was used to solve the

thermal model. The temperature-dependent data range is limited by measurement capabilities and assumed to remain constant above the indicated temperature range. The dashed lines show the temperature-time profiles measured using thermocouples located at the heated surface, middle and unheated surface of the composite. The solid lines show the profiles calculated using Eqn. (1). The agreement between the measured and calculated temperatures is good for 10, 25 and 50 kW/m$^2$ over the entire range of heating times. Smouldering of the composite occurred at these heat fluxes, but the polymer matrix did not ignite and burn. The agreement is also good for 75 kW/m$^2$ up to 200 s, but at longer times the measured temperatures are much higher. The disagreement occurs because the polymer matrix ignited at 200 s causing flaming combustion. This accelerated the decomposition rate that in turn increased the measured temperature. The thermal model cannot capture the ignition event, and therefore the calculated temperatures are too low.

Based on this analysis it appears that the thermal model can predict the temperature-time response of the fibreglass composite for any heat flux and heating time up to the onset of flaming combustion. Once the composite ignites and experiences sustained flaming combustion, there is a rapid increase in the temperature due to a rise in the decomposition rate of the polymer matrix. Therefore the thermal-mechanical model is only valid for hot, smouldering composites that do not ignite and burn.

### 4.2 High Temperature Strength of Fibreglass, Polymer Matrix and Composite

This section presents the analysis and strength data for the fibreglass, matrix and composite under isothermal conditions, but not the fire conditions, which are presented in the next section.

The tensile strength of the fibreglass reinforcement must be calculated using Eqn. (11) before the tensile strength of the composite can be determined using the thermal-mechanical model. Values for the empirical constants of $k_{fb}(T)$ and $p_{fb}$ have to be determined from tensile strength data for glass fibres measured at different temperatures and times. Relatively few studies have been published on the effects of temperature [19] and heating time [16,20] on the tensile strength of E-glass fibres, so it was decided to measure the reduction in tensile strength of the fibreglass for different heating

conditions to determine the values for $k_{fb}(T)$ and $p_{fb}$. This is a labour intensive exercise, but it only needs to be done once as the fitted values are assumed to be similar for any type of E-glass fibre. The bundle size and effect of friction between fibres are assumed to be of minimal importance.

Figure 7 shows the effect of temperature and heating time on the normalised tensile strength of E-glass fibre bundles. The strength of the heat-treated fibres is normalised to their original (as-received) room temperature bundle strength, which was 125 N. Variations in fibre strength led to average strength values above 100% prior to strength reduction, although the standard deviation indicates that no statistically significant changes were measured. As expected, the strength decreases with increasing temperature (above ~150$^{o}$C) and time. The curves follow the shape of the *tanh* function described by Eqn. (5). Using the nonlinear least-squares Marquardt-Levenberg fitting algorithm in Gnuplot, the parameters in Table 2 were obtained for the fibre bundles. Apart from the value for $k_1$, which describes the rate of strength decrease, all parameters show a low standard error. The standard error should not be used to determine confidence levels, but is useful for qualitative purposes to determine the goodness of the fitting function. The large error for $k_1$ indicates that better fitting functions could be found. Equally, more data points might reduce the fitting error further. Alternatively, additional data points might reveal a slightly different trend for which a different fitting function to Eq. (6) would be more appropriate. It should be noted that $T_{50\%}$,, the temperature at which the fibre bundle strength is reduced by 50%, is 347ºC and is therefore much lower than the annealing or softening temperature of E-glass, which is typically around 650ºC. Figure 8 presents a tensile strength-temperature-time plot comparing the measured strength values with the strength curve calculated using Eqn. (5), and the agreement is excellent. This demonstrates that the fitting function gives a good prediction of the change in fibre strength.

The effect of temperature on the tensile strength of the vinyl ester is shown in figure 9 (a). The strength decreases rapidly between 50 and 150ºC, and this due to the glassy transition of the polymer network structure. Above 150ºC, only a very small fraction of the original strength remains. Many other polymer systems show a similar relationship between strength and temperature, which can be

described by the hyperbolic *tanh* function given in Eqn. (4). The curve in figure 9 (a) is fitted using this equation. The compressive strength of the composite laminate follows the same trend [15], and the respective experimental data points were included in the fit to increase the number of data points. The calculated material constants are summarised in Table 3.

Figure 9(b) shows the tensile strength reduction of the glass/vinyl ester composite with increasing temperature. The strength reaches a minimum at about 180ºC and then remains constant up to 300ºC. For the short term exposure during composite testing, the loss of fibre strength remains at a minimum under these conditions, as seen in figure 7, while the matrix has fully softened at these temperatures. Using this data, the following values for the composite system are established at room temperature: $V_f$ = 0.28 (in load direction), $\sigma_{m(0)}$ = 69 MPa, $\sigma_{fb(0)}$ = 1800 MPa and $\Phi_{SL}$ = 1. The resin softening parameters derived in figure 9(a) are applied. The resin is found to contribute about 10% to the room temperature composite strength when applying Eqn. (12), which clearly over-predicts the remaining composite strength. The fibre bundle strength (1800 MPa) is below the pristine glass fibre strength (2800 MPa). This is attributed to the (1) fibre bundle effect and (2) use of woven glass fabric that contains twisted and crimped fibres. Solving Eqn. (13) at temperatures above 180ºC results in a load transfer factor of $\Phi_{LT}$ = 0.8. It is assumed that $\Phi_{LT}(T)$ at lower temperatures follows the same softening curve as the resin itself. Eqn. (13) is plotted in figure 9(b) and is shown to give an accurate prediction of the experimental data. While $\Phi_{LT}$ has a physical meaning, its simplistic use in Eqn. (13) results in a fitted material value valid only for the specific material system and specimen geometry.

### 4.3 Tensile Modelling of Fibreglass in Fire

The thermal-mechanical model was used to calculate the time-to-failure of fibreglass fabric (without the polymer matrix) when exposed to one-sided heating at a constant flux. Fire-under-load tests were performed on the fibreglass fabric used as the reinforcement in the vinyl ester composite. The tests involved subjecting a 15-ply fabric laminate to combined tensile loading and one-sided heating at the heat flux of 50 kW/m$^2$. Tensile stresses from 20% to 80% of the original rupture strength (at 20$^o$C)

were applied to the fabric laminate during heating. Tests were performed with and without thermal insulation on the unheated surface of the fabric specimens. This was done to evaluate the model for two temperature conditions: (1) the insulated case that generated high internal temperatures and (2) non-insulated case that involved lower temperatures due to convective cooling from the unheated surface. Temperature-time profiles measured at different locations through the specimens are shown in figure 10, and as expected the insulation increased the heating rate and maximum internal temperatures because heat loss by convection from the back surface was minimised.

Figure 11 shows the effect of applied tensile load on the time-to-failure of the fabric with and without insulation. The normalised load is the applied tensile load during heating divided by the tensile rupture load of the fabric specimen at 20$^{o}$C, which is 125 kN. The data points show the experimental failure times, and as expected they increase when the applied load is reduced. At very low loads the fabric laminate did not fail after two hours, and it is assumed to have an infinite survival time. These data points showing when failure did not occur are within the box labelled 'run-out'. The failure times are much longer, particularly at low loads, when the fabric laminate was not insulated because the internal temperature is lower. Figure 10 shows that a steady-state temperature condition is reached after ~600 s and 1000 s for the non-insulated and insulated specimens, respectively. The fabric strength, however, continues to decrease beyond these times. This suggests that time-dependent or creep processes control the rupture strength and time-to-failure of the fabric laminate at long heating times.

The reduction to the average tensile strength of the fabric laminate during the fire-under-load tests can be calculated using Eqn. (14), ignoring the effect of the polymer matrix. Once the average strength is calculated it is then possible to determine the time-to-failure of the fabric. The failure time is the heating time required for the calculated tensile strength to decrease to the applied tensile load, at which time failure must occur. The curves in figure 11 show the predicted relationship between failure time and applied tensile stress, and there is good agreement with the experimental results for both the insulated and non-insulated fabrics. Run-outs of the specimens after two hours are also predicted

correctly. It is worth noting that the model fails to address one important issue: Stress rupture of the fibres due to slow crack growth under load, also known sometimes as delayed failure. The fibre strength reduction was determined on unstressed fibres exposed to various heating times, while the fire-under-load tests heat fibres while under constant load. Stress rupture can further lower the failure times.

### 4.4 Tensile Modelling of Fibreglass Composites in Fire

The thermo-mechanical model is validated using time-to-failure values of a glass/vinyl ester composite tested at a range of heat fluxes. The specimen gauge length is much larger ($l$ = 560 mm) than the specimen used previously to establish the elevated temperature data in figure 9(b) ($l$ = 150 mm). As a consequence, the room temperature strength is reduced from 545 MPa to 470 MPa because of a size effect in fibre strength and load transfer. The matrix strength is assumed to remain constant, although it should be noted that its contribution is minor in evaluation of Eq. (13). The loss of load transfer, on the other hand, plays an important role in the reduction of composite strength. Re-evaluation of the tensile strength data according to Eqn. (13) yields a reduced fibre bundle strength ($\sigma_{fb}$) of 1530 MPa and an increased load transfer factor ($\Phi_{LT}$) of 0.88 for this specimen size, which are used in the following calculations. A more advanced model for tensile strength predictions of a woven composite could include the effect of specimen size on the material parameters.

The data points in figure 12 are the experimental failure times used to validate the model. This figure shows that the failure times increase rapidly when the tensile stress applied to the composite is reduced. As expected, the failure times also increase by reducing the heat flux. When the applied stress and heat flux are sufficiently low the composite did not fail, and these tests were run-out after several hours. Similar trends to that shown in figure 12 have been measured for other fibreglass composites, including glass/polyester and glass/phenolic materials [11]. The solid curves show the relationship between failure time and applied load calculated using the thermal-mechanical model (Eqn. (14)), and there is reasonable agreement with the experimental data. The curves show a four-stage reduction in tensile strength: (I) relatively small decrease (of ~20%) at short times, (II) a short-

term stabilisation immediately following stage I, (III) large reduction at intermediate times, and (IV) a constant low strength at long times. The four stages are indicated on the curve for the heat flux of 75 $kW/m^2$.

The initial reduction in strength at high loads during stage I is due to thermal softening of the polymer matrix. The model predicts that the tensile strength of the matrix will decrease within a short time due to its low softening temperature. The model also correctly predicts that the reduction in strength due to matrix softening will occur more slowly at lower heat fluxes. The curves show that the initial reduction in strength occurs over a period of about 100 s at 75 $kW/m^2$, and this time increases with decreasing heat flux to about 300 s at 10 $kW/m^2$. The curves show the tensile strength stabilises at a constant value of 80% of the room temperature strength for a brief period before dropping again. The strength stabilises for a short time in stage II because the polymer matrix has reached a fully softened state but the fibre strength has not yet been changed significantly by the heating. This corresponds to the reduced strength at elevated temperature around 150 to 300ºC as shown in figure 9 (b). The model predicts a large reduction in strength in stage III due to softening of the glass fibres, and this is confirmed by the experimental data. However, the curves under-estimate the failure times of the composite, with the discrepancy becoming greater when the heat flux is reduced. The model predicts that the strength of the composite will reach a minimum constant value after prolonged heating (stage IV). The composite will not fail when the applied stress is below this residual strength value, and this was confirmed by the fire-under-tests that were 'run-out' under low load, low heat flux conditions. This comparison between the theoretical failure curves and experimental data reveals that the thermal-mechanical model can predict the various softening stages of a composite and give a conservative estimate of the failure time.

## 5 CONCLUSIONS

The thermo-mechanical model can predict the tensile strength and estimate the failure time of fibreglass fabric and fibreglass-polymer composites exposed to fire with a constant radiant heat flux. The model considers thermal softening of the polymer matrix due to the glassy transition and

decomposition. Thermal softening of the polymer matrix reduces slightly the tensile strength of fibreglass composites when initially exposed to fire, but eventually has no significant affect once the matrix is fully softened and decomposed. The model also considers thermal softening of the glass reinforcement, which is dependent on both the temperature and heating time. The model shows that tensile failure of fibreglass composites is controlled mostly by fibre softening. The model can accurately predict the tensile strength and failure time of fibreglass fabric laminates, although it gives an approximation of the tensile strength of fibreglass-vinyl ester composites, particularly under low load and low heat flux conditions. While this study has shown that the model gives a good estimate of the tensile strength and failure time for vinyl ester composites, further validation of the model is required for other fibreglass-polymer systems. Once the model is thoroughly validated it is envisaged it can be used to predict the tensile properties and aid in the design of composite structures used in high fire risk applications.

**ACKNOWLEDGEMENTS**

This research was performed as part of a research project (P2.1.1) within the Cooperative Research Centre for Advanced Composite Structures (CRC-ACS). The study was funded by the United States Office of Naval Research (Grant No. N00014-04-10026) under the direction of Dr L. Couchman. One of us, AGG, would like to acknowledge the support of the UK EPSRC for his contribution to this work. The authors thank Peter Tkatchyk (RMIT) for constructing the fire-under-load test apparatus and for assistance when conducting the tests. The technical assistance of Sarina Russo (DSTO) in measuring the temperature-time response of the laminates is also acknowledged. The authors would furthermore like to thank Colan Products Ltd for the supply of glass fibres for the project.

**REFERENCES**

1 McManus, H.L.N. and Springer, G.S. (1992). High-temperature thermomechanical behavior of carbon-phenolic and carbon-carbon composites: 1. Analysis. *Journal of Composite Materials*, **26**: 206-229.

2 Sullivan, R.M. (1993). A coupled solution method for predicting the thermostructural response of decomposing, expanding polymeric composites. *Journal of Composite Materials*, **27**: 408-434

3 Wu, Y. and Katsube, N. (1997). A thermomechanical model for chemically decomposing composites. 1. Theory. *International Journal of Engineering Science*, **35**: 113-128

4 Dao, M. and Asaro, R.J. (1999). A study on failure prediction and design criteria for fiber composites under fire degradation. *Composites*, **30A**: 123-131.

5 Asaro, R.J., Krysl, P. and Ramroth, W.T. (2006). Structural fire integrity of FRP composites: analysis and design., In: Couchman, L. and Mouritz, A.P. (ed.), *Modeling of Naval Composite Structures in Fire*, Acclaim Printing, Melbourne, pp. 301-327.

6 Bausano, J., Boyd, S., Lesko, J. and Case, S. (2003). Composite life under sustained compression and one-sided simulated fire exposure: Characterization and prediction. In: *Proceedings of Composites in Fire-3*. 9-10th September, University of Newcastle-upon-Tyne, UK.

7 Boyd, S.E., Bausano, J.V., Case, S.W. and Lesko, J.J. (2006). Mechanistic approach to structural fire modeling of composites. In: Couchman, L. and Mouritz, A.P. (ed.), *Modeling of Naval Composite Structures in Fire*, Acclaim Printing, Melbourne, pp. 201-258.

8 Liu, L., Holmes, J.W., Kordomateas, G.A. and Birman, V. (2006). Compressive response of composites under combined fire and compression loading. In: Couchman, L. and Mouritz, A.P. (ed.), *Modeling of Naval Composite Structures in Fire*, Acclaim Printing, Melbourne, pp. 109-142.

9 Lua, J. and O'Brien, J. (2003). Fire simulation for woven fabric composites with temperature and mass dependent thermal-mechanical properties. In: *Proceedings of Composites in Fire-3*. 9-10th September, University of Newcastle-upon-Tyne, UK.

10 Gibson, A.G., Wu, Y.S., Evans, J.T. and Mouritz, A.P. (2004). Laminate theory analysis of composites under load in fire. *Journal of Composite Materials*, **38**: 1283-1307.

11 Mouritz, A.P., Feih, S., Mathys, Z. and Gibson, A.G. (2006). Mechanical property degradation of naval composite materials in fire. In: Couchman, L. and Mouritz, A.P. (ed.), *Modeling of Naval Composite Structures in Fire*, Acclaim Printing, Melbourne, pp. 51-108.

12 Gibson, A.G., Mouritz, A.P. and Mathys, Z. (2004). The integrity of polymer composites during and after fire. *Journal of Composite Materials*, **38**:1283-1306.

13 Gibson, A.G., Wu, Y-S., Chandler, H.W., Wilcox, J.A.D. and Bettess, P. (1995). A model for the thermal performance of thick composite laminates in hydrocarbon fires. *Revue de L'Institut Francais du Petrole*, **50**: 69-74.

14 Henderson, J.B., Wiebelt, J.A and Tant, M.R. (1985). A model for the thermal response of polymer composite materials with experimental verification. *Journal of Composite Materials*, **19**: 579-595.

15 Feih, S., Mathys, Z., Gibson, A.G. and Mouritz, A.P. (in press). Modelling the compression strength of polymer laminates in fire. *Composites A*.

16 Gupta, P.K. (1988). ‘Glass fibers for composite materials’, Chapter 2 of *Fibre Reinforcements for Composite Materials*, ed. Bunsell, A.R., Elsevier, New York, 1988.

17 Baker, A., Dutton, S. and Kelly, D. (2004). Composite Materials for Aircraft Structures. AIAA, ISBN 1-56347-540-5

18 Looyeh, M.R.E. and Bettess, P. (1998). A finite element model for the fire-performance of GRP panels including variable thermal properties. *Finite Elements in Analysis and Design*, **30**: 313-324

19 AGY technical paper. ‘High strength Glass Fibers’, Pub. No. LIT-2004-011 R1, 2004, USA

20 Thomas, W.F. (1960). An investigation of the factors likely to affect the strength and properties of glass fibres. *Physics and Chemistry of Glasses*, **1**: 4-18

*Table 1: Thermal property data for the vinyl ester / glass composite.*

| **Property** | **Value** | **Source** |
|---|---|---|
| Rate constant, *A* [1/s] | 5.59E13 | TGA [$N_2$] |
| Activation energy, *E* [J/(kg mol)] | 212705 | TGA [$N_2$] |
| Order of decomposition reaction, *n* | 1 | TGA [$N_2$] |
| Remaining Resin Mass Fraction [%] | 3.0 | TGA [$N_2$] |
| Heat of decomposition [J/kg] | 378800 | DSC/TGA [$N_2$] |
| Specific heat glass/vinyl ester [J/(kg K)] (45ºC) | 960.0 | DSC |
| Specific heat glass/vinyl ester [J/(kg K)] (140ºC) | 1210.0 | DSC |
| Specific heat glass/vinyl ester [J/(kg K)] (290ºC) | 1360.0 | DSC |
| Specific heat gas [J/(kg K)] | 2386.5 | Literature [18] |
| Thermal conductivity glass /vinyl ester [W/(m K)] (60-300ºC) | 0.43 | In-house test |
| Fibre volume fraction | 0.55 | In-house test |

*Notes: TGA = thermogravimetric analysis*
*DSC = differential scanning calorimetry*

*Table 2: Fitted data for glass fibre strength reduction*

| Values | Fitted value | Standard error [%] |
|---|---|---|
| $T_{50\%}$ [ºC] | 347.6 | 3.9 |
| $p_{fb}$ [ºC$^{-1}$] | 5.83E-3 | 11.1 |
| $k_1$ [s$^{-1}$] | 1.81E-6 | 58.2 |
| $k_2$ [ºC$^{-1}$] | 1.45E-2 | 8.8 |

*Table 3: Fitted data for resin and compressive composite strength reduction*

| Values | Fitted value | Standard error [%] |
|---|---|---|
| $k_m$[ºC$^{-1}$] | 0.026 | 11.5 |
| $T_g$' [ºC] | 88 | 3.3 |

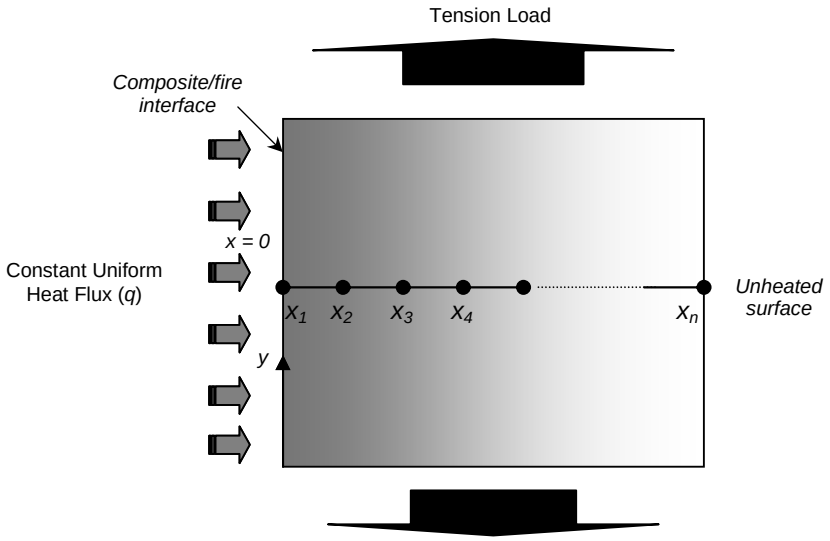


Figure 1. Schematic of a composite beam under combined axial loading and one-sided heating.

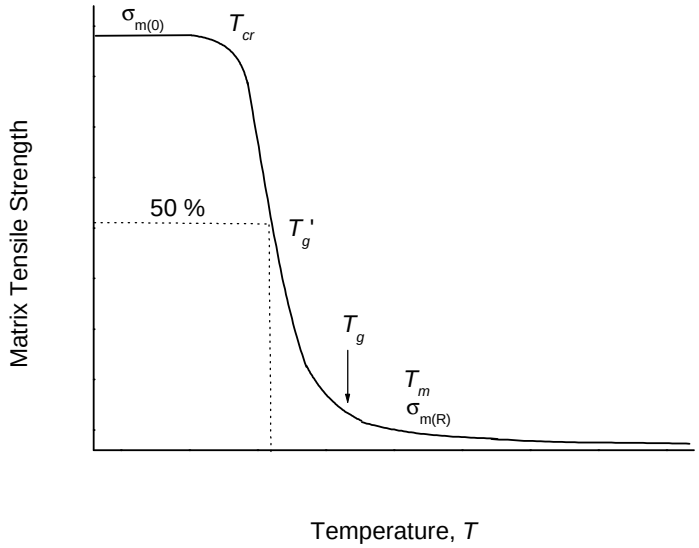


Figure 2. Representation of the typical relationship between temperature and tensile strength of a polymer.

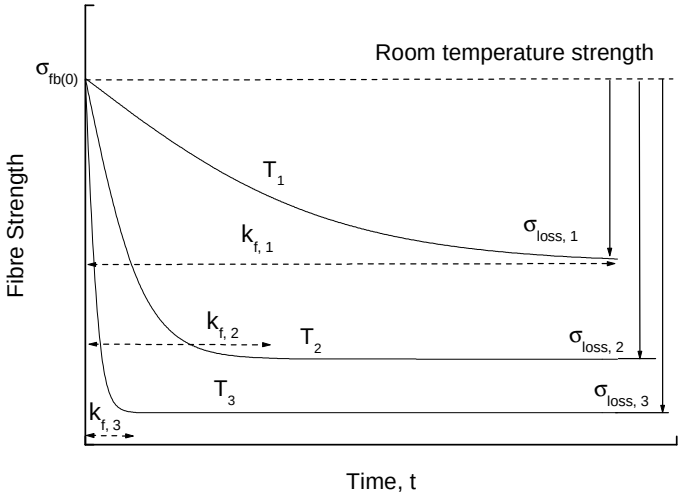


(a) Isothermal fibre strength reduction

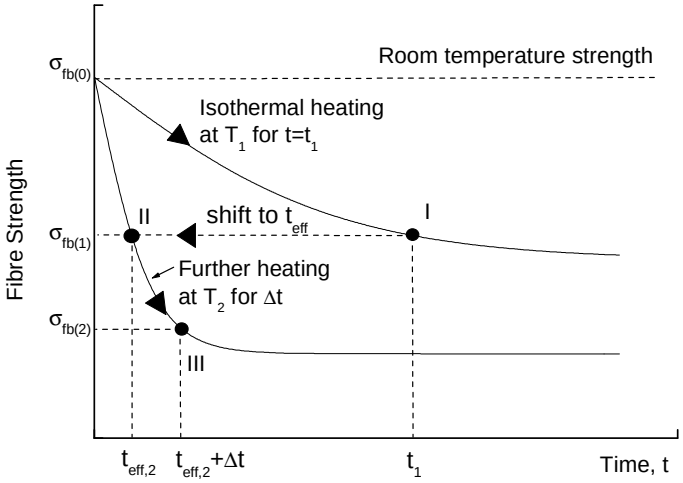


(b) Fibre strength reduction during non-isothermal heating

Figure 3. Representation of (a) the typical relationship between temperature, time and tensile strength of glass fibres, (b) algorithm for non-isothermal strength degradation

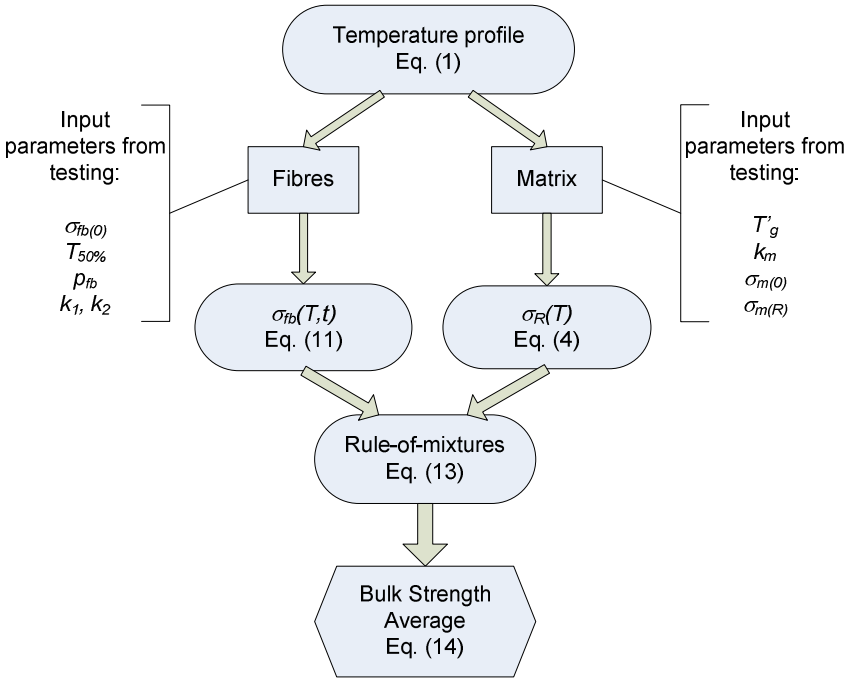


Figure 4. Schematic flow chart of analytical algorithm to calculate tensile strength during fire

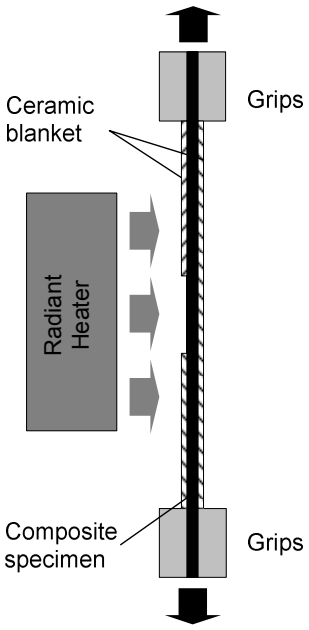


Figure 5. Schematic of the fire-under-test.

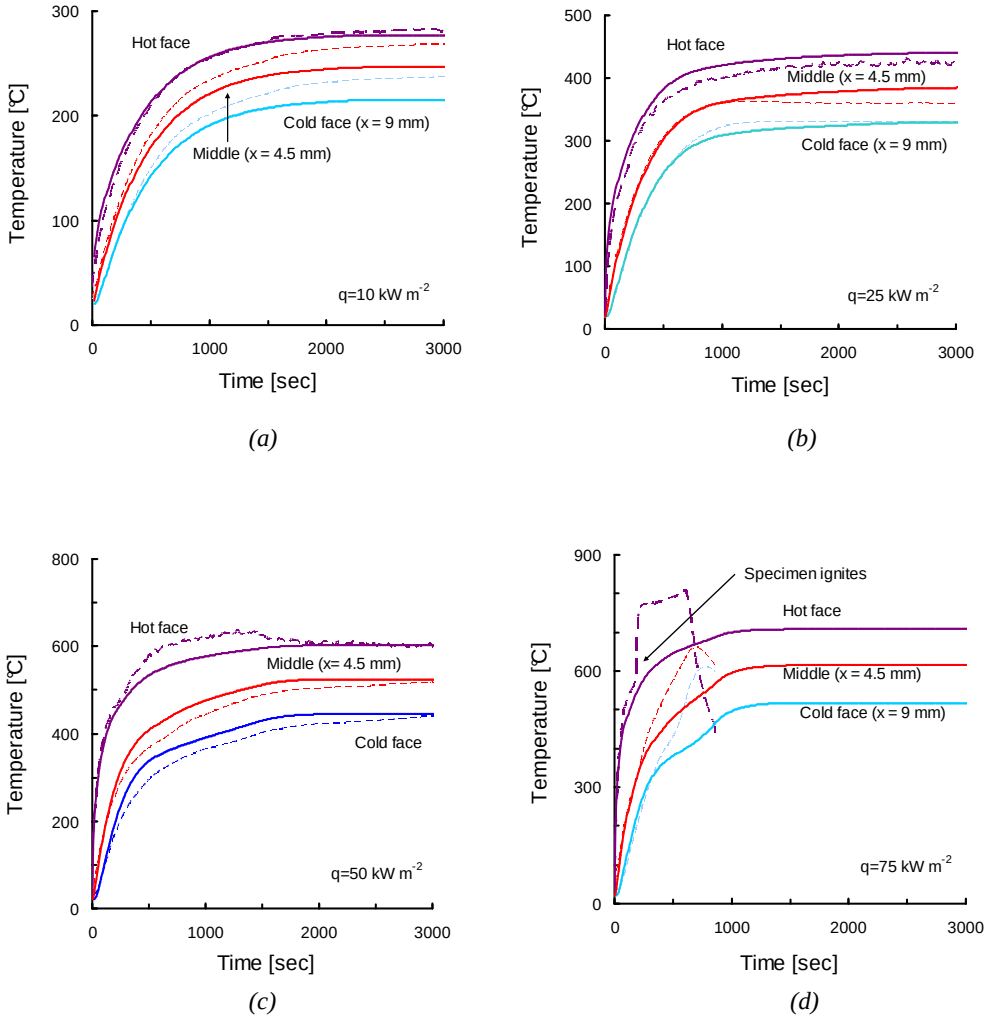


Figure 6. Temperature-time profiles through the glass/vinyl ester laminate at heat fluxes of (a) 10, (b) 25, (c) 50 and (d) 75 kW/m$^2$. The measured and calculated temperatures are shown by the dashed and solid curves, respectively.

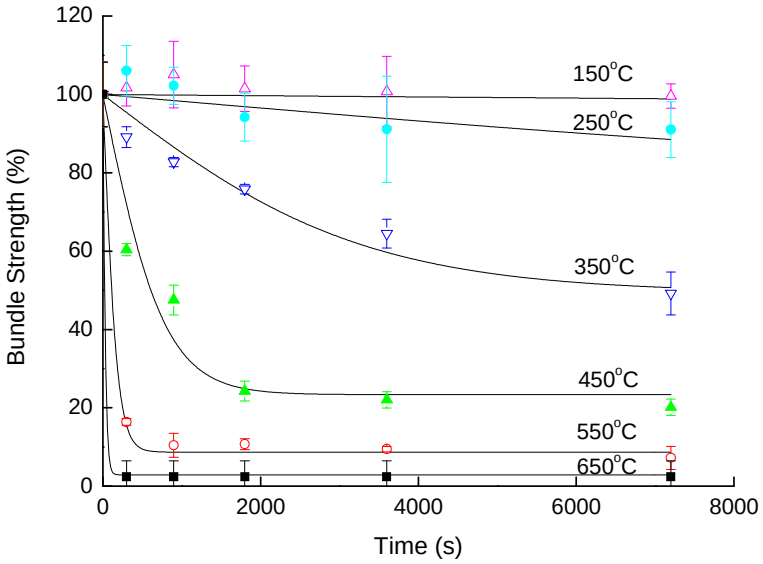


Figure 7: Experimental results for fibre strength as a function of time and temperature.

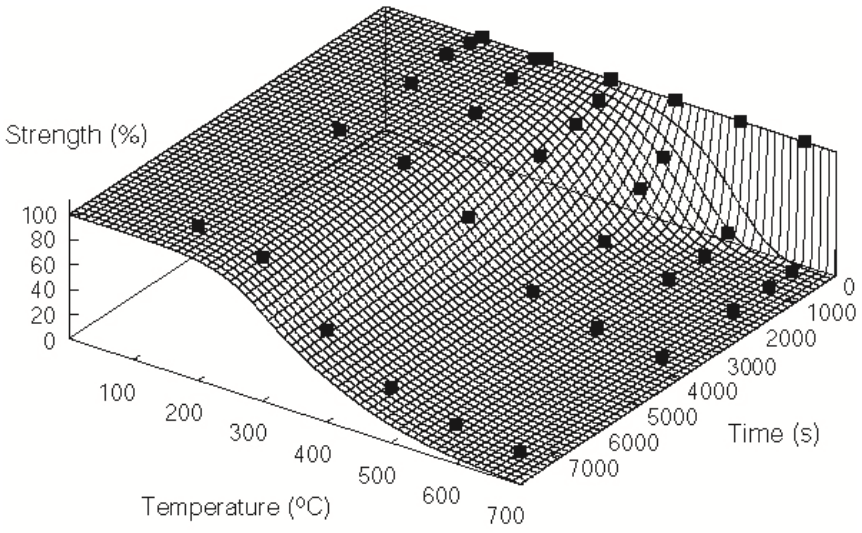


Figure 8: 3D plot of fitted glass strength data.

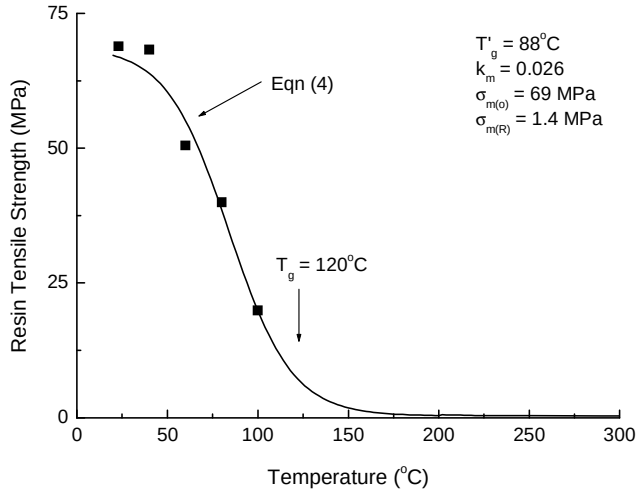


(a)

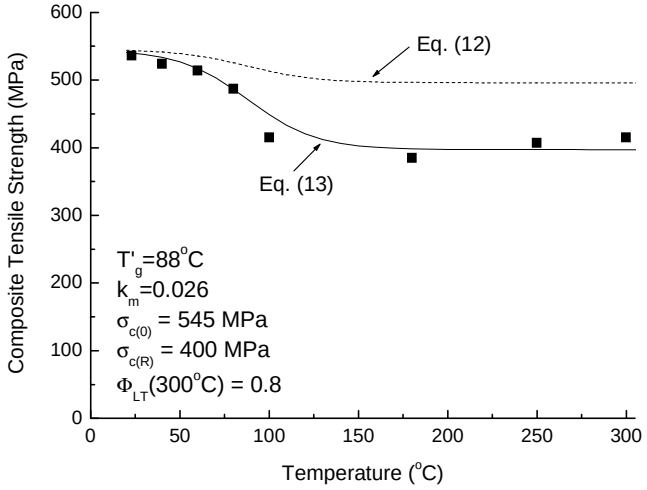


(b)

Figure 9: Effect of temperature on the tensile strength of (a) vinyl ester and (b) vinyl ester / glass composite. Heat exposure is short term with about 10 minutes to minimise glass strength reduction.

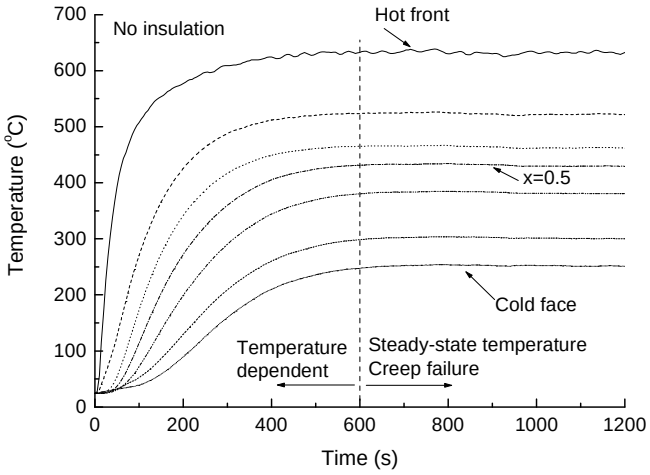


*(a)*

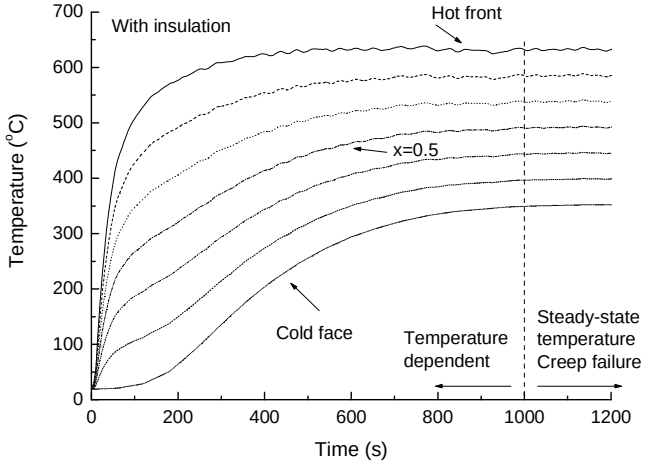


*(b)*

Figure 10: Temperature profiles for glass only laminates with (a) no insulation and (b) back face insulation

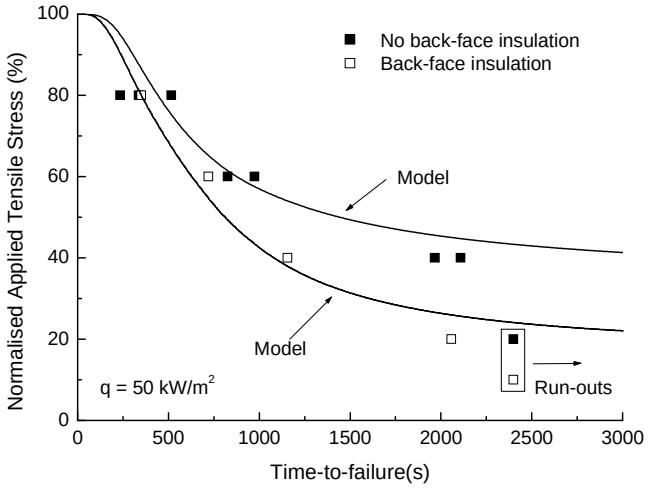


Figure 11: Predicted time-to-failure for dry glass laminates.

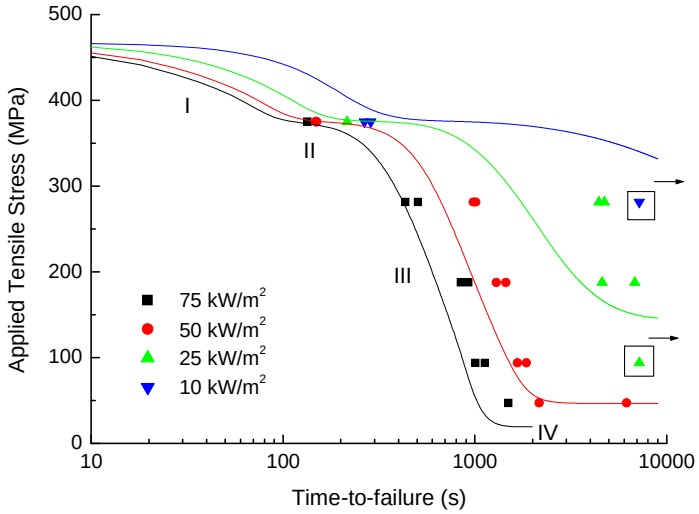


Figure 12: Predicted time-to-failure for glass / vinyl ester laminates including resin load transfer degradation.